Journal of the European Ceramic Society **17** (1997) 921–928

PII: S0955-2219(96)00164-1
0955-2219/97/$17.00

SiC Nanoparticle-Reinforced Al_2O_3 Matrix Composites: Role of Intra- and Intergranular Particles

Youren Xu,[a] Avigdor Zangvil[a,*] & Albert Kerber[b]

[a]Materials Research Laboratory, University of Illinois at Urbana-Champaign, Urbana, Illinois 61801, USA
[b]LONZA-Werke GmbH, D-7890 Waldshut-Tiengen, Germany

(Received 1 July 1994; revised version received 26 July 1996; accepted 5 August 1996)

Abstract

Submicron (or 'nanocrystalline') SiC-reinforced Al_2O_3 matrix composites have been prepared by co-milling followed by hot-pressing at 1650°C. Both intra- and intergranular SiC particles were present. The volume ratio for intra- to intergranular particles was approximately 30 : 70 for 6 vol% SiC composites and 20 : 80 for 12 vol% SiC composites. The intragranular SiC (50–200 nm) formed mainly by growth of the Al_2O_3 matrix grains, while Zener pinning, mainly by the larger (200–300 nm) particles, was thought to effectively limit the Al_2O_3 grain size. Approximately 15% toughening was achieved by incorporating 12 vol% SiC nanoparticles into the matrix. The intergranular particles provided most of the toughening, mainly through a SiC particle-attracted crack deflection mechanism and crack impediment. No evidence was found of toughening by the intragranular particles, although they did cause some grain refinement by dislocation sub-boundary formation. A mixed fracture mode was observed, changing to a mostly intergranular mode with increasing volume of SiC particles. © 1997 Elsevier Science Limited.

1 Introduction

Nanocomposites, having a ceramic matrix reinforced with submicron (nanosized) particles (up to several hundred nanometers in size), have emerged as a new class of materials. Significant results have been reported on SiC nanoparticle-reinforced Al_2O_3 matrix composites by Niihara *et al.*, who measured 1 GPa bending strength for an Al_2O_3 matrix reinforced with 5 vol% SiC particles with a size of 0·3 μm.[1] Further results were presented in later publications, where bending strength as high as 1·5 GPa was achieved by annealing at 1300°C for 1 h in air or inert atmosphere.[2–4] The fracture toughness was also reported to increase from 3·25 MPa $\sqrt{m}$ for the monolithic Al_2O_3 material to 4·70 MPa $\sqrt{m}$ for a 5 vol% SiC particle/Al_2O_3 composite.[1] Intragranular-type nanocomposites were emphasized in this system, where ~200 nm SiC particles were located mainly within Al_2O_3 grains, while some other SiC particles (mostly larger in size) were observed at grain boundaries.[1–4] The strengthening was attributed to intragranular particle-induced dislocations which further develop to subgrain boundaries, resulting in a matrix grain refinement. The toughening was believed to be due to crack tip deflection by the hard inclusions.

Recently, Zhao *et al.* initiated a discussion regarding the achievement of high strength/toughness in Al_2O_3–SiC nanocomposite.[5] They claimed that the high strength can only be achieved by surface grinding and annealing, which greatly reduce the intrinsic flaw size of samples. Using the strength-indentation method, they calculated that the addition of the SiC particles does not increase the intrinsic material toughness, and concluded that the observed toughening in these materials is almost entirely from compressive surface stresses induced by the grinding process. No distinction has been made in their paper between the functions of intra- and intergranular particles, although the intra-type SiC particles were clearly the main feature in the composites. A transgranular fracture mode was found in this system, but no toughening has been achieved. Their explanation was that the enhanced toughness by SiC particle-induced transgranular fracture is compensated by the decrease in toughness due to cracks passing through the tensile stress fields between second-phase and matrix particles.[5]

*Also with the Department of Materials Science and Engineering, UIUC.

It is the purpose of the present study to further investigate the microstructural features in this system, mainly the role of intra- and intergranular particles in microstructural evolution and in the toughening process. Toughening due to intergranular sub-micron particles (as opposed to intragranular particles in previous studies) is of particular interest. It is expected that the acquired basic understanding of dominant mechanisms of toughening and the corresponding desirable microstructures would be utilized in the development of novel composite materials with improved mechanical properties.

2 Experimental Procedure

Low-soda alumina (α structure, CS-400M, Martinswerke, Begheim, Germany) with a mean particle size of 0·6 μm, and ultra-fine silicon carbide (α structure, UF-15, LONZA-Werke, Germany) with a mean particle size of 0·5 μm were used in the present study. Five and 10 wt% (approximately equal to 6 and 12 vol%, respectively) SiC particles were added to the Al_2O_3 starting powder (resulting in compositions L_6 and L_{12}) and the mixtures were co-milled in water for 3 h. After co-milling, the particle size distribution of both L_6 and L_{12} mixtures was as follows: 100% <0·7 μm, d_{90} = 0·42 μm, d_{50} = 0·29 μm and d_{10} = 0·19 μm. The specific surface area measured by the BET method was 48 $m^2\ g^{-1}$. The powder mixtures were poured into a graphite die, where graphite foil was used to avoid contact between the die and the powders. The samples were hot-pressed at 1650°C for 1 h under a mechanical pressure of 40 MPa in a flowing argon atmosphere (1 atm). The fracture toughness was determined using an indentation technique.[6–8] Samples for the indentation test were cut from hot-pressed billets with the testing surface oriented parallel to the hot-pressing direction. Surfaces were ground on diamond disc through 30 to 15 μm, then polished to a 1-μm-diamond finish. Vickers diamond pyramid indentations were made on polished specimens using a 100-N indentation load to ensure radial cracks and hardness impressions of reasonable dimensions (total crack length > twice the indent diagonal in all cases). At least nine indents were made on each sample. Fracture toughness, K_{1c}, was calculated by the following equation:[8]

$$K_{1c} = \xi(E/H)^{1/2}(P/c^{1/2}) \quad (1)$$

where E is Young's modulus, H is Vickers hardness, P is the contact load and c is the crack length, measured from the center of the contact impression. The material-independent, dimensionless calibration constant ξ, which is determined by the geometry of the deformation field, was selected as 0·016.[8]

Microstructural characterization was performed on commercial transmission electron microscopes (Models EM 420 and CM-12, Philips Electronic Instruments, Eindhoven, the Netherlands). Samples for the TEM study were prepared by the usual procedures for ceramics, i.e. slicing, disc cutting, mechanical grinding/polishing, dimpling, and ion milling. To avoid serious charging in the TEM, a thin layer of carbon was deposited on the thin foil. Indentation crack propagation observations were carried out on a scanning electron microscope (S-800, Hitachi Ltd, Japan). Samples for this study were first polished to 1-μm-diamond finish, then indented with several 60–90 N indents on the polished surface, and finally thermally etched at 1300°C for 30 min in a vacuum furnace. A thin layer of Au–Pd coating was applied to enhance the electrical conductivity of the indented surface.

The lineal intercept technique[9] was applied to determine the grain size of Al_2O_3 matrix by multiplying the average linear length of at least 100 grains by 1·56, using the following formula:

$$\bar{D} = 1{\cdot}56\,\frac{C}{MN} \quad (2)$$

where $\bar{D}$ is the average grain size, C the total length of test line used, N the number of intercepts, and M the magnification of the photomicrograph.

3 Results and Discussion

3.1. General microstructural features

Figure 1 shows the general microstructural features of samples L_6 and L_{12}, with 6 and 12 vol% SiC particles, respectively. The average grain size of the Al_2O_3 matrix was 1·7 ± 0·9 μm for L_6 and 1·3 ± 0·7 μm for L_{12}, respectively. The second-phase (SiC) particle size varied from ~50 to 300 nm. The dispersion of the second-phase particles was in two forms: intragranular and intergranular. The volume ratio for intra- to intergranular particles was approximately 30 : 70 for the 6 vol% SiC composite and decreased to approximately 20 : 80 as SiC particle volume was increased to 12%. Generally, the intragranular particles were small, ranging from 50 to 200 nm, while the intergranular particles were larger, from 200 to 300 nm. Some abnormally grown Al_2O_3 grains, which were usually 5 μm or more in size, could be found in sample L_6. The same phenomenon was observed in L_{12} (with a higher volume fraction of SiC), but

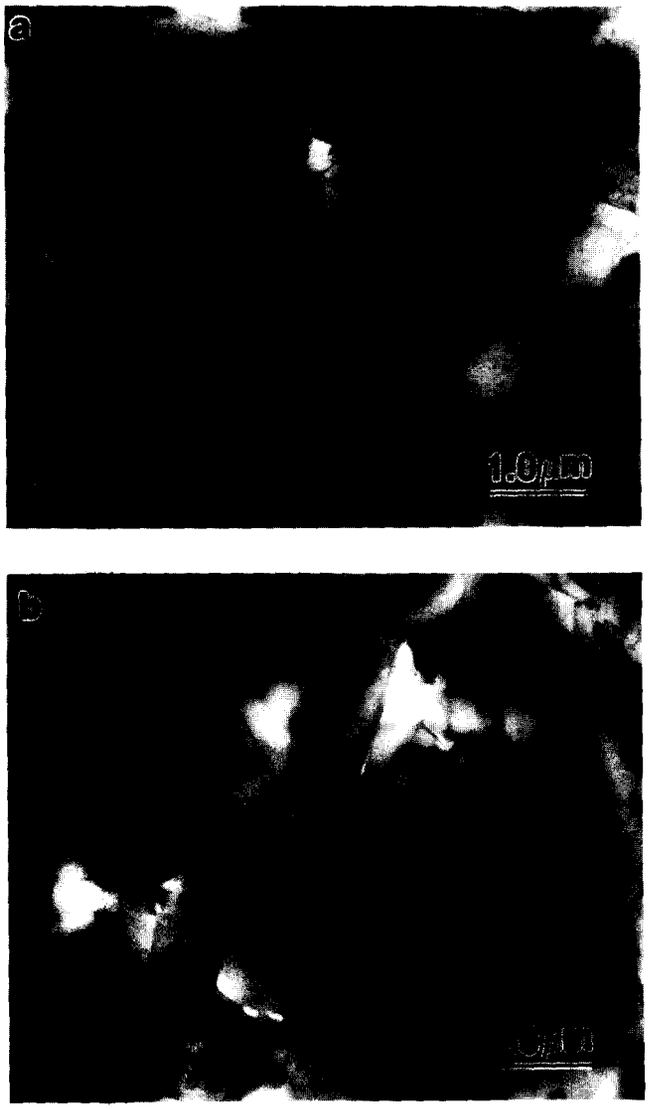

Fig. 1. Microstructure of Al_2O_3–SiC nanocomposites: (a) sample L_6 with 6 vol% SiC; (b) sample L_{12} with 12 vol% SiC.

the amount and size of the abnormally grown grains were less than in sample L_6. All the abnormally grown Al_2O_3 grains typically contained many small SiC inclusions, as shown in Fig. 2, where many SiC particles (most of them with size of ~100 nm) were trapped by an abnormally grown Al_2O_3. It seems that considerable grain growth, which is known to occur in Al_2O_3 during sintering at temperatures > 1550°C,[10] happens in our composites only in some locations, where larger SiC particles are not present.

3.2. Pinning by second-phase particles

In contrast to Al_2O_3, grain growth of the strongly covalently bonded SiC is not expected at the present hot-pressing temperature of 1650°C, and certainly not when only widely separated particles are present. Once Al_2O_3 grains begin growing (involving grain-boundary migration), these second-phase SiC particles can either be pinning grain boundaries or be dragged by grain boundaries.[10–13] The boundary drag, however, requires that the

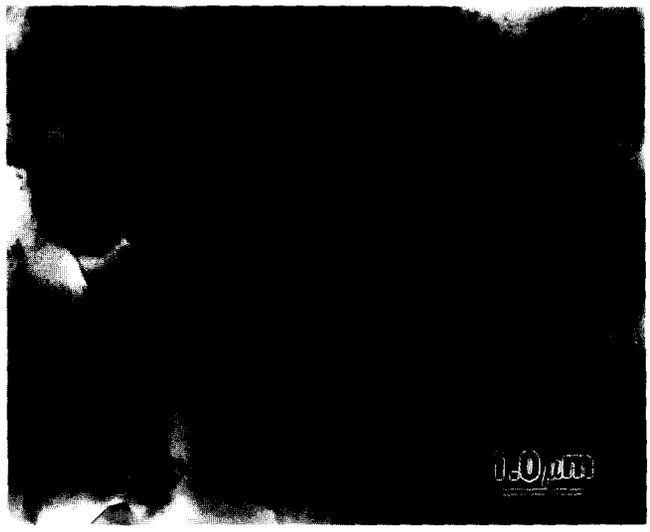

Fig. 2. TEM image showing many intragranular SiC particles within an abnormally grown Al_2O_3 grain (sample L_6).

inclusion move with the boundary through interfacial diffusion or volume diffusion,[13,14] which needs the inclusion to have sufficient self-diffusion. It seems that this process occurs with difficulty in the present system because the sintering temperature for SiC is >1950°C (with small additions of sintering aids and/or with application of high pressure[15]), which is much higher than that for Al_2O_3 (1300 ~ 1600°C[10]), and no sufficient self-diffusion can be expected for SiC at 1650°C. Therefore, pinning would be more likely in the present system. When the grain boundary reaches a particle, the boundary energy will decrease by a value proportional to the cross-sectional area of the particle. A breakaway stress will then have to be applied in order to release the boundary from the pinning particle. Clearly, the smaller particles provide less effective pinning than the larger ones. They will be more likely to become inclusions as shown in Figs 1 and 2, because the decrease of the boundary energy is small, and boundaries can easily break away from them. Conversely, larger particles tend to remain at grain boundaries because they significantly decrease the boundary energy, requiring larger breakaway stresses.

The Zener pinning of grain boundaries[11] is generally accepted as explaining inhibition of grain growth by inclusions. Applying Zener pinning to a real system requires assumption that second-phase particles are (1) spherical; (2) of equal size; and (3) of random distribution. An important but often confused point in these assumptions is the random distribution, which means that second-phase particles can be randomly located both at boundaries and within grains. This assumption raises an important issue: Zener pinning takes no account of the initial grain growth, because all the second-phase particles are located at grain

boundaries before grain growth and, therefore, are not distributed randomly. After an initial grain growth, however, the inclusions can be considered to be more randomly distributed (because now we are considering a larger scale), and Zener pinning models may be applied. In the initial stage, all particles (assuming a uniform particle size) interact with grain boundaries and affect the grain growth. Using computer simulation, Hazzledine and Oldershaw established an equation, which is valid for volume fractions $f > 1\%$:[16]

$$D/d = (6/f)^{1/3} \quad (3)$$

where D and d are the grain sizes of matrix and second phase, respectively.

The assumption of equal size particles is not valid in our samples. Observations that particles with sizes of ~50–100 nm are usually trapped within matrix grains indicate that grain boundaries are easy to break away from small particles since their cross-sectional area is much smaller than that of 200–300 nm particles. Their contribution to pinning can therefore be neglected, as a rough approximation. The volume fraction of particles ≤ 100 nm in size is estimated at about 20%. This would suggest an 'effective volume fraction' of second-phase particles of ~80% of the total volume fraction or about 4·8% for L_6 and 9·6% for L_{12}. Using this approximation and the intergranular particle size only (200–300 nm), we get D = 1·0–1·5 μm for L_6 and D = 0·8–1·2 μm for L_{12}, very close to the observed Al_2O_3 grain sizes (1·7 ± 0·9 μm in L_6 and 1·3 ± 0·7 μm in L_{12}). The fact that the Zener-predicted grain sizes are somewhat smaller than the actual ones is not surprising. It can be explained by the non-random distribution of particles (e.g. large local concentrations of particles are a 'waste' in terms of pinning and make pinning less effective), and by the far-from-ideal grain shapes, particle shapes, etc.

3.3. Role of intra- and intergranular particles in toughening

Table 1 shows the fracture toughness values of the Al_2O_3–SiC nanocomposites and monolithic Al_2O_3. It is clear that the fracture toughness of Al_2O_3–SiC nanocomposites (4·70–4·85 MPa √m) is higher than that for the monolithic Al_2O_3 ceramics (~4·20 MPa √m), although there is no significant change in K_{Ic} when SiC volume fraction increases from 6% to 12%. These results are somewhat lower than previous published values,[1–4] but still show 12–15% toughening compared to the presently measured K_{Ic} for monolithic Al_2O_3, and ~45% increase over the literature-reported K_{Ic} for monolithic Al_2O_3.[1,17]

Table 1. Fracture toughness of Al_2O_3–SiC nanocomposites and monolithic Al_2O_3

Material	*Fracture toughness (MPa √m)*
Al_2O_3	4·20 ± 0·10
L_6 (6% SiC)	4·70 ± 0·11
L_{12} (12% SiC)	4·85 ± 0·03

Extensive SEM observation of the indentation-generated crack propagation showed that the cracks were more likely to propagate through matrix grain boundaries containing a higher than average density of intergranular SiC particles. Figure 3(a) shows the SEM image of indentation crack propagation in sample L_6. As can be seen, the crack was deflected by a large Al_2O_3 grain into its boundary, which contained several SiC particles. A similar phenomenon was found in sample L_{12}, as shown in Fig. 3(b), where the crack was attracted by the intergranular particle without

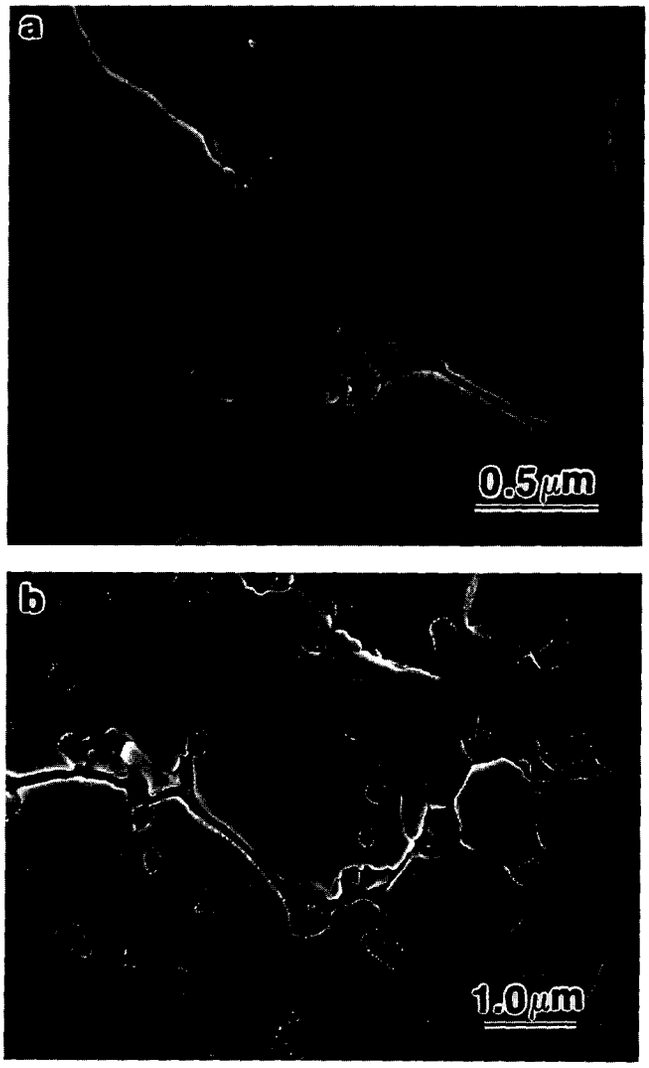

Fig. 3. SEM images of indentation crack propagation in (a) sample L_6, showing that the crack was attracted by several SiC particles around a large Al_2O_3 grain, resulting in a significant crack deflection; (b) sample L_{12}, the crack was preferentially attracted by the intergranular SiC particle without interacting with intragranular particles.

interacting with intragranular particles (even though some intragranular particles were on the original propagation direction of the crack). The crack is attracted to the intergranular particle due to the formation of a tensile residual stress field around the particle and perpendicular to the adjacent boundary, because of the large negative thermal expansion mismatch between the SiC particle ($\alpha = 4{\cdot}7 \times 10^{-6}{}^{\circ}C^{-1}$) and the Al_2O_3 matrix ($\alpha = 8{\cdot}8 \times 10^{-6}{}^{\circ}C^{-1}$), and this will increase crack deflection length at least to some extent (selective propagation) compared to the normal intergranular propagation of the crack in monolithic alumina (non-selective propagation). This process should lead to a high incidence of crack impediment events (by the hard SiC particles), contributing to toughness. The crack can also be deflected by the intergranular particle itself when the size of the particle is large enough as shown in Fig. 4, where a significant crack deflection was made by an ~1-μm long intergranular particle. This should provide a small, but still meaningful, increment to the toughness.

Interactions between cracks and intragranular particles were much less frequent. When such a case occurred, it was associated with either a larger intragranular particle (Fig. 5(a)) or an agglomeration of inclusions (Fig. 5(b)). This would suggest that the transgranular propagation of the crack occurs only when a relatively high tensile residual stress field forms due to the presence of a large SiC intragranular particle within the matrix grain. However, we did not find any evidence of the crack deflection by intragranular particles as suggested by Niihara *et al.*[1-4] Another mechanism observed by Niihara *et al.* is the grain refinement through subgrain boundary formation by nanocrystalline inclusions.[1-4] We did find a subgrain boundary which developed from intragranular particle-induced dislocations, as shown in Fig. 6. However, it was a rare occurrence, and certainly not a dominant phenomenon which could provide matrix grain refinement for strengthening. Our findings about the role of intra- and intergranular particles in toughening are different from those of Niihara *et al.*, where the toughening was attributed to crack deflection toward SiC *intragranular* particles.[1-4] The result of Zhao *et al.*,[5] namely that no toughening could be obtained in an Al_2O_3–SiC nanocomposite material with mostly intragranular inclusions, seems to support our conclusion, although their explanation may still be considered questionable. At any rate, we believe that the intragranular particles do not make a significant contribution to the fracture toughness of our materials, because (1) less transgranular fracture was observed in the high SiC composite (L_{12}) which has a higher fracture toughness than the low SiC sample (L_6); (2) no consistent correlation was found between the amounts of transgranular

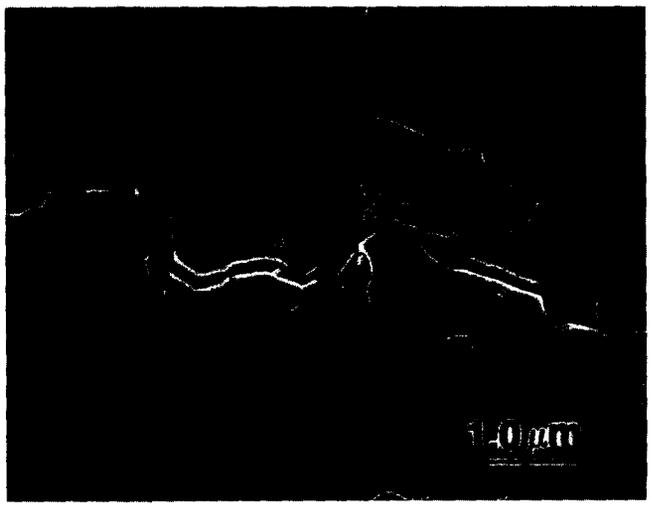

Fig. 4. SEM image showing a significant crack deflection was caused by an ~1-μm-long intergranular SiC particle (sample L_{12}).

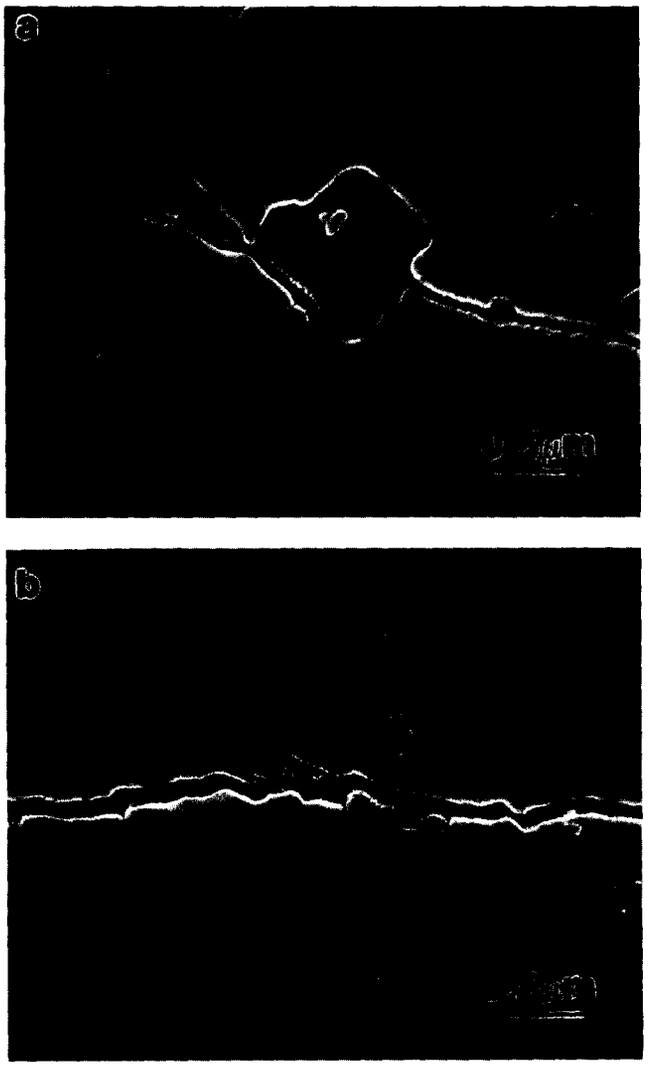

Fig. 5. Intragranular particle-induced transgranular fracture was usually associated with either (a) a larger intragranular particle or (b) an agglomeration of inclusions, suggesting that a relatively high tensile residual stress field was required for the crack to propagate through the matrix grain.

Fig. 6. TEM micrograph (dark field image) showing the intragranular particle-induced dislocations developing into a microcrack (sample L_6).

fracture and intragranular particles in individual grains; (3) less crack deflection can be provided by the intragranular particle (no tendency for the crack to be attracted by the intragranular particle, and the crack usually propagates straight within the Al_2O_3 grain); (4) the intragranular particles were 20–30% of the total second-phase particles, so their volume fraction was only 2–3% even in the 12% SiC sample.

These facts, along with the observation of crack interaction with the grain boundary particles, lead to the conclusion that toughening in our system is mainly due to intergranular particles. This is achieved by (1) Zener pinning causing reduced grain size; (2) crack attraction into certain grain boundary paths by particles; (3) crack impediment by the intergranular particles; and (4) crack path extension due to deflection around large intergranular particles. In our composites, the majority of SiC second phase is present in the form of intergranular particles, while most SiC particles dispersed as inclusions within matrix grains in nanocomposites processed by both Niihara *et al.* and Zhao *et al.* The SiC particle size in our composites (average of 0·20–0·25 μm) is not much different from those of Niihara *et al.* or Zhao *et al.* However, grain growth inhibition was more effective in our materials, probably due to differences in processing conditions and/or raw materials, resulting in a higher fraction of intergranular particles.

4 Fracture Mode

The fracture mode in monolithic alumina is intergranular, and is promoted by residual tensile microstresses. These stresses exist at some grain boundaries of polycrystalline alumina because of thermoelastic anisotropy. Adding SiC to form intragranular particles has two main effects on fracture mode: (1) creation of local compressive stresses on adjacent grain boundaries, thus strengthening boundaries and decreasing the total probability of intergranular fracture; and (2) formation of a tensile residual stress field within the matrix grain (around the particles) because of the large thermal expansion mismatch with the SiC particles, and if this field is large enough it will deflect the crack toward the intragranular particle and away from the grain boundaries, resulting in a transgranular fracture.[19] Both Niihara *et al.* and Zhao *et al.* have found that adding 5 vol% SiC nanoparticles can change the fracture mode in Al_2O_3 from intergranular to transgranular.[1–5] The fracture surface of the present composites has been studied in detail by SEM, and results are shown in Fig. 7. Sample L_6 (Fig. 7(a)) exhibited regions typical of an intergranular fracture, as well as cleavage steps indicative of a transgranular fracture. Sample L_{12} (Fig. 7(b)) showed a much smaller amount of transgranular fracture. This suggests that in our materials the ratio of transgranular to intergranular fracture does not increase with increasing volume of SiC nanoparticles, and that a critical volume of SiC nanoparticles should exist to achieve maximum transgranular fracture. Beyond this limit, the tendency for *transgranular* fracture (due to intragranular inclusions) is more than offset by the increasing amount of intergranular SiC, which inhibits the grain growth of Al_2O_3 and weakens grain boundaries due to the formation of tensile residual stresses. Such a weakening by intergranular particles not only promotes intergranular fracture but also provides toughening by impeding cracks and/or by increasing the crack deflection length. During the revision of the present manuscript, more papers discussing strengthening and toughening by 'nanoscale' SiC particles, were published in the literature.[18,19] A calculation based on a simple model of Al_2O_3–SiC (intragranular) nanocomposites indicated that the toughening by the change in fracture mode from intergranular to transgranular can be achieved only for low (less than 6 vol%) SiC contents, while a high SiC volume will result in high tensile residual stresses which will significantly decrease the fracture toughness.[19] In a study of SiC nano-dispersion in Si_3N_4 matrix composites (no sintering additives), no strengthening and toughening were claimed.[18] The present work on Al_2O_3–SiC nanocomposites, which has focused on clarifying the role of intra- and intergranular SiC dispersion on the toughening process, is a

Fig. 7. SEM images of the fracture surface of samples (a) L_6 and (b) L_{12}. The amount of transgranular fracture in the high SiC composite (L_{12}) was much smaller than in the low SiC sample (L_6).

complementary study to meet the growing interest in this subject. The difference in results between the present work and previous studies conducted by Niihara *et al.*[1–4] as well as recent reports[5,18,19] is probably due to the different microstructural nature of our materials — an intergranular particle-dominated nanocomposite.

5 Conclusions

(1) Dispersed SiC second phase is present in the form of both intra- and intergranular particles in the Al_2O_3–SiC nanocomposites. The volume ratio for intra- to intergranular particles was approximately 30 : 70 for 6 vol% SiC composites and 20 : 80 for 12 vol% SiC composites. The particle size of the inclusions (mostly 50–100 nm) is generally smaller than that of the intergranular grains (200–300 nm). The occurrence of the intragranular SiC within matrix grains is caused by the grain growth of Al_2O_3, and the abnormal grain growth of Al_2O_3 results in an additional increase of the fraction of intragranular particles.

(2) Zener pinning can be postulated for the 1650°C hot-pressed Al_2O_3–SiC nanocomposites, where the Al_2O_3 grain growth was effectively inhibited by the larger second-phase SiC particles. The pinning behavior was generally consistent with Hazzledine and Oldershaw's expression $D/d \approx 1{\cdot}82\, f^{-1/3}$.

(3) Modest toughening was achieved in the present materials. Crack impediment and crack attraction into certain grain boundary paths by intergranular particles, as well as crack deflection by large intergranular particles appeared to be the main toughening mechanisms. No evidence was found for substantial contribution to the fracture toughness from the intragranular particles, although they did cause some grain refinement by dislocation sub-boundary formation.

(4) The high volume of SiC particles in our composites (≥ 6 vol%) as well as processing facts caused the formation of intergranular SiC-dominated nanocomposites, which demonstrated (a) different toughening mechanisms from previous studies, and (b) a partly intergranular fracture mode, as opposed to the fully transgranular fractures seen in other studies.

Acknowledgements

This work is supported by the US Department of Energy, Division of Materials Sciences, under Grant No. DE-FG02-91ER45439. Microanalysis was carried out in the Center for Microanalysis of Materials, University of Illinois, which is supported by the same grant.

References

1. Niihara, K. and Nakahira, A., Strengthening of oxide ceramics by SiC and Si_3N_4 dispersions. In *Proceedings of the Third International Symposium on Ceramic Materials and Components for Engines*, ed. V. J. Tennery. The American Ceramic Society, Westerville, OH, 1988, pp. 919–926.
2. Niihara, K., Sekino, T., Nakahira, A. and Hirano, T., Fabrication and mechanical properties of ceramic based composites with nono-sized ceramic and metal dispersions. In *Abstracts of the 96th Annual Meeting of the American Ceramic Society*, Indianapolis, IN, April 1994. Paper No. SIII-54-94, p. 36.

3. Niihara, K. and Nakahira, A., Particulate strengthened oxide nanocomposites. In *Advanced Structural Inorganic Composites*, ed. P. Vincenzini. Elsevier Scientific Publishing Co., Trieste, 1990, pp. 637–664.
4. Niihara, K., New design concept of structural ceramics—Ceramic nanocomposites. The Centennial Issue of the Ceramic Society of Japan. *J. Ceram. Soc. Jpn*, 1991, **99**, 974–982.
5. Zhao, J., Stearns, L. C., Harmer, M. P., Chan, H. M. and Miller, G. A., Mechanical behavior of alumina–silicon carbide 'nanocomposite'. *J. Am. Ceram. Soc.*, 1993, **76**, 503–510.
6. Lawn, B. R. and Fuller, E. R., Equilibrium penny-like cracks in indentation fracture. *J. Mater. Sci.*, 1975, **10**, 2016–2024.
7. Evans, A. G. and Charles, E. A., Fracture toughness determinations by indentation. *J. Am. Ceram. Soc.*, 1976, **59**, 371–372.
8. Anstis, G. R., Chantikul, P., Lawn, B. R. and Marshall, D. B., A critical evaluation of indentation techniques for measuring fracture toughness: I. Direct crack measurements. *J. Am. Ceram. Soc.*, 1981, **64**, 533–538.
9. Wurst, J. C. and Nelson, J. A., Lineal intercept technique for measuring grain size in two-phase polycrystalline ceramics. *J. Am. Ceram. Soc.*, 1972, **55**, 109.
10. Lange, F. F. and Hirlinger, M. M., Hindrance of grain growth in Al_2O_3 by ZrO_2 inclusions. *J. Am. Ceram. Soc.*, 1984, **67**, 164–168.
11. Zener, C., quoted by Smith, C. S., Grains, phases, and interfaces: an interpretation of microstructure. *Trans. Am. Inst. Min. Metall. Engrs*, 1948, **175**, 15–51.
12. Brook, R. J., Controlled grain growth. In *Treatise on Materials Science and Technology*, vol. 9, ed. F. F. Wang. Academic Press, New York, 1976, pp. 331–364.
13. Ashby, M. F. and Centamore, R. M. A., The dragging of small oxide particles by migrating grain boundaries in copper. *Acta. Metall.*, 1968, **16**, 1081.
14. Shewman, P. G., Movement of small inclusions in solids by a temperature gradient. *Trans. Metall. Soc. AIME*, 1964, **230**, 1134–1137.
15. Prochazka, S., The role of boron and carbon in the sintering of SiC. In *Special Ceramics*, Vol. 6, ed. P. Popper. British Ceramic Research Association, Manchester, UK, 1975, pp. 171–182.
16. Hazzledine, P. M. and Oldershaw, R. D. J., Computer simulation of Zener pinning. *Phil. Mag., A*, 1990, **61**, 579.
17. Smith, S. M. and Singh, J. P., Processing and characterization of SiC-whisker-reinforced alumina-matrix composites. *J. Am. Ceram. Soc.*, 1992, **76**, 497–502.
18. Pezzotti, G. and Sakai, M., Effect of a silicon carbide 'nano-dispersion' on the mechanical properties of silicon nitride. *J. Am. Ceram. Soc.*, 1994, **77**, 3039–3041.
19. Levin, I., Kaplan, W. D., Brandon, D. G. and Layyous, A. A., Effect of SiC submicrometer particle size and content on fracture toughness of alumina-SiC nanocomposites. *J. Am. Ceram. Soc.*, 1995, **78**, 254–256.